*Satellites and Tidal Streams*
*ASP Conference Series, Vol. **VOLUME***, 2003*
*F. Prada, D. Martínez-Delgado, and T. Mahoney, eds.*



# Dark Matter in Dwarf Galaxies: Latest Density Profile Results

Joshua D. Simon, Alberto D. Bolatto, Adam Leroy, and Leo Blitz

*Department of Astronomy, University of California at Berkeley, 601 Campbell Hall, CA 94720*

**Abstract.** We present high-resolution two-dimensional velocity fields in H$\alpha$ and CO of the nearby dwarf galaxy NGC 2976. Our observations were made at both higher spatial resolution ($\sim$ 75 pc) and higher velocity resolution (13 km s$^{-1}$ in H$\alpha$ and 2 km s$^{-1}$ in CO) than most previous studies. We show that NGC 2976 has a very shallow dark matter density profile, with $\rho(r)$ lying between $\rho \propto r^{-0.3}$ and $\rho \propto r^{0}$. We carefully test the effects of systematic uncertainties on our results, and demonstrate that well-resolved, two-dimensional velocity data can eliminate many of the systematic problems that beset longslit observations. We also present a preliminary analysis of the velocity field of NGC 5963, which appears to have a nearly NFW density profile.

## 1. Introduction

It is well-known by now that there is a substantial disagreement between the observed dark matter density profiles of many dwarf and low-surface brightness galaxies and the density profiles predicted by numerical Cold Dark Matter (CDM) simulations (e.g., Flores & Primack 1994; Burkert 1995; Navarro, Frenk, & White 1996, hereafter NFW; Moore et al. 1999). The significance of this disagreement, though, remains controversial. A number of authors attribute the problem to failures of the simulations, or of the CDM model itself (de Blok et al. 2001a; de Blok, McGaugh, & Rubin 2001b; Borriello & Salucci 2001; de Blok, Bosma, & McGaugh 2003), while others argue that systematic uncertainties in the observations make such conclusions premature (van den Bosch et al. 2000; van den Bosch & Swaters 2001; Swaters et al. 2003, hereafter SMVB).

We address this controversy with a new study that combines a number of techniques to overcome the systematics in the observations. We are acquiring very high-quality data on a limited sample of galaxies to investigate the importance of systematic effects in detail. The results of this study should make clear whether systematic problems in the data are at fault, or whether there actually is a fundamental conflict between the theory and the observations.

Our program includes (1) two-dimensional velocity fields obtained at optical (H$\alpha$), millimeter (CO), and centimeter (H I) wavelengths, (2) high angular resolution ($\sim 5''$), (3) high spectral resolution ($\lesssim$ 10 km s$^{-1}$), (4) multicolor optical and near-infrared photometry, and (5) nearby dwarf galaxies as targets.

The combination of these features greatly reduces our vulnerability to systematic uncertainties (see Simon et al. 2003).

In two previous papers, we reported on rotation curve studies of the dwarf spiral galaxies NGC 4605 and NGC 2976 (Bolatto et al. 2002; Simon et al. 2003). In this paper we highlight some of those results, focusing on tests for systematic uncertainties in the NGC 2976 data set, and we also present preliminary results on the third galaxy in our study, NGC 5963.

## 2. The Dark Matter Halo of NGC 2976

NGC 2976 is a regular Sc dwarf galaxy located in the M81 group at a distance of 3.45 Mpc. The galaxy has absolute magnitudes of $M_B = -17.0$ and $M_K = -20.2$, and a total mass of $3.5 \times 10^9 M_\odot$; it is somewhat less luminous and less massive than the Large Magellanic Cloud. In optical and near-infrared images it is clear that NGC 2976 is a bulgeless, unbarred, pure disk system, which makes it an ideal galaxy for mass modeling.

### 2.1. Observations

Our observations of NGC 2976 include a two-dimensional H$\alpha$ velocity field (obtained with a multi-fiber spectrograph on the WIYN telescope), a two-dimensional CO velocity field (obtained with the BIMA interferometer), multi-color optical photometry, and near-infrared 2MASS imaging. The velocity fields are both shown in Figure 1. For details of the data reduction and analysis, see Simon et al. (2003).

### 2.2. Rotation Curve

We used various tilted-ring modeling algorithms to convert the observed velocity field into a rotation curve (see Simon et al. 2003). The rotation curve of NGC 2976 is well-described by a single power law from the center of the galaxy out to a radius of almost 2 kpc, as displayed in Figure 2a. The rotation curve only begins to deviate systematically from power law behavior at $r \approx 110''$ (1.84 kpc). The *total* (baryonic plus dark matter) density profile corresponding to the rotation curve is $\rho_{\rm TOT} = 1.6(r/1\ {\rm pc})^{-0.27\pm0.09} M_\odot\ {\rm pc}^{-3}$. Because the baryons are almost certainly centrally concentrated, this density profile represents the cuspiest possible shape for the dark matter halo.

### 2.3. Dark Matter Density Profile

To explore the full range of possible dark matter density profile slopes, we must account for the rotational velocities contributed by the baryonic components of the galaxy. Because our images of NGC 2976 do not reveal a bulge or a bar, and its nucleus is dynamically unimportant, the only relevant reservoirs of baryons to consider are the stellar and gaseous disks. We calculated the rotation curves due to the stars and gas directly from the observed surface density profiles, assuming an infinitely thin disk. The only free parameter in these calculations is the K-band mass-to-light ratio of the stellar population ($M_*/L_K$).

Under the assumption that the density profile can be described with a power law, $\rho_{\rm DM} \propto r^{-\alpha_{\rm DM}}$, we found that if $M_*/L_K > 0.19 M_\odot/L_{\odot K}$, $\alpha_{\rm DM} < 0$ and the

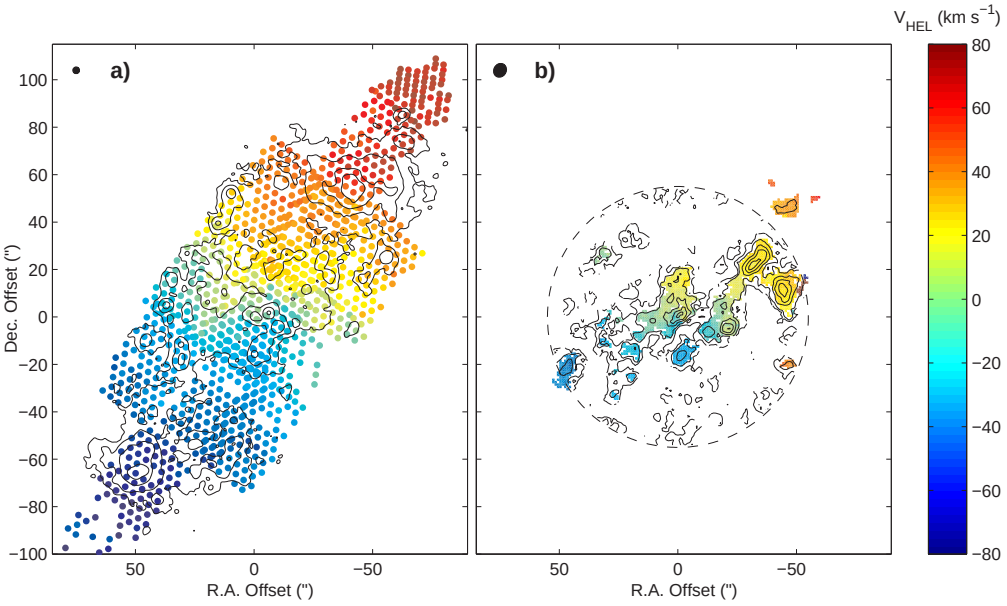


Figure 1. (a) H$\alpha$ velocity field of NGC 2976 from WIYN observations. The contours represent integrated H$\alpha$ intensity. (b) CO velocity field from BIMA observations. The contours represent integrated CO intensity. The angular resolution of each dataset is shown in the upper left corners.

density of the dark matter halo is increasing with radius. Such a dark matter configuration is probably unphysical, so we consider 0.19 $M_{\odot}/L_{\odot K}$ to be a firm upper limit to the stellar disk mass-to-light ratio, with the corresponding lower limit to $\alpha_{\rm DM}$ of 0. Because of the extremely low value of the maximal disk mass-to-light ratio, the galaxy must contain an essentially maximal disk. The dark matter density profile for the maximal disk is $\rho_{\rm DM} = 0.1(r/1\ {\rm pc})^{-0.01\pm0.13} M_{\odot}\ {\rm pc}^{-3}$. This represents the most likely shape for the dark matter halo. Since the slope of the total density profile of the galaxy represents the absolute upper limit for the slope of the dark matter density profile, we conclude that the dark matter density profile is bracketed by $\rho_{\rm DM} \propto r^{-0.27\pm0.09}$ and $\rho_{\rm DM} \propto r^{0}$.

## 3. Systematics

Several authors have recently discussed the systematic uncertainties that can significantly alter observed rotation curves. SMVB used simulated observations to argue that systematic effects alone could account for the difference between the predicted and observed density profile slopes. de Blok et al. (2003) carried out similar simulations, but concluded that the systematic effects were not strong enough to cause cuspy density profiles to appear to have cores. We have shown that, *for the specific case of NGC 2976*, the known systematic problems do not distort the rotation curve (Simon et al. 2003; this work). The worst systematics can probably be minimized or avoided *in general* by using two-

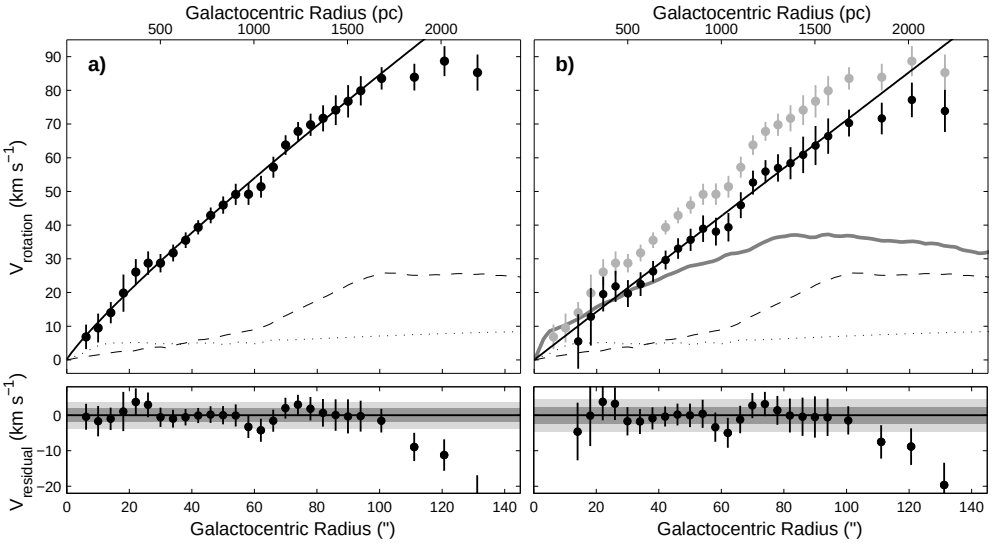


Figure 2. (a) Minimum disk rotation curve of NGC 2976. The observed rotation velocities are plotted as black circles and the error bars are combined statistical and systematic uncertainties. The dashed and dotted curves represent the rotation velocities due to H I and $H_2$, respectively. A power law fit to the rotation curve is shown by the solid black curve. The corresponding density profile is $\rho \propto r^{-0.27}$. Residuals from the fit are displayed in the lower panel, and $1\sigma$ and $2\sigma$ departures from the fit are represented by the shaded regions. (b) Maximum disk rotation curve of NGC 2976. The stellar disk (thick gray curve) is scaled up as high as the observed rotation velocities (gray circles) allow. The stellar disk shown here has $M_*/L_K = 0.19\ M_\odot/L_{\odot K}$. After subtracting the rotation velocities due to the stars and the atomic and molecular gas from the observed rotation curve, the dark matter rotation velocities are displayed as black circles. The two missing data points near the center of the galaxy had $v_{rot} < v_{*,rot}$, yielding imaginary $v_{halo}$. The solid black line is a power law fit to the halo velocities (for $14'' < r < 105''$) which corresponds to a density profile of $\rho_{\rm DM} \propto r^{-0.01}$. The halo residuals after the power law fit are displayed in the bottom panel.

dimensional velocity fields and by making velocity measurements at very high precision (Blais-Ouellette et al. 1999; van den Bosch & Swaters 2001; Bolatto et al. 2002; SMVB), but additional observations confirming this expectation for more galaxies are needed.

### 3.1. Rotation Curve Fitting Systematics

Because of the high precision of our velocity measurements, the statistical uncertainties on both the rotation curve and the radial velocity curve are negligible (less than 1 km s$^{-1}$ everywhere). Therefore, the limiting factors on the accuracy of the rotation curve are the systematic uncertainties associated with our fit.

*Uncertainties in Geometric Parameters* Before computing the uncertainties on the rotation velocities themselves, we must first determine the uncertainties on each of the parameters that are used to calculate the rotation velocities: the center, position angle (PA), inclination, and systemic velocity. We used a bootstrap resampling technique to calculate the value and uncertainty of these parameters. We constructed 200 bootstrap samples of the velocity field and ran our tilted-ring modeling routine (RINGFIT) on each of them to determine the best-fit kinematic center. We then defined the center of the galaxy to be the median of these 200 measurements, and the systematic uncertainty on the center position to be the dispersion of the measurements. We found that the location of the kinematic center of NGC 2976 is consistent with the optical nucleus, with an uncertainty of $2''$ in both $\alpha$ and $\delta$. We used the same bootstrap method to measure the kinematic PA of the galaxy and its uncertainty, finding that the kinematic PA matches the photometric one and has an uncertainty of $5^\circ$. It is not possible to determine a kinematic inclination angle for NGC 2976 because the rotation curve is too close to solid-body. However, the photometric inclination angle is well determined, and we estimate that the uncertainty is $3^\circ$.

The uncertainty in the systemic velocity was calculated in a different way. The systemic velocity of each ring was left free to vary during our tilted-ring fitting, resulting in 23 independent measurements. The overall uncertainty from these measurements is 1.8 km s$^{-1}$. Since $v_{sys}$ is always a free parameter, this uncertainty does not directly factor in to the uncertainty on the rotation curve.

*Uncertainties in Rotation Velocities and Radial Velocities* Using the measured uncertainties in the center position, PA, and inclination angle, we calculated the resulting uncertainties on the rotation velocities and the radial velocities with a Monte Carlo study. We generated 1000 random centers, PAs, and inclinations, assuming a Gaussian distribution for each of the parameters, and ran RINGFIT with each set of parameters. The standard deviation of the 1000 rotation velocities in each ring was defined to be the systematic error of that rotation velocity, and the systematic errors in the radial velocities and systemic velocities were calculated in the same way. The systematic errors on the rotation curve range from 2.1 km s$^{-1}$ to 5.5 km s$^{-1}$. The sum in quadrature of these errors and the statistical errors translates to a total uncertainty on the density profile slope $\alpha$ of 0.09. We conclude that, even in the minimum disk case, an NFW or steeper density profile in NGC 2976 is strongly ruled out.

### 3.2. Other Systematic Effects

In some studies, beam-smearing is one of the dominant systematic effects. The velocity field of NGC 2976, though, is extremely well-resolved — our spatial resolution is less than 100 pc in both CO and H$\alpha$. The measured velocity gradient is small ($\sim$ 50 km s$^{-1}$ kpc$^{-1}$) and the constant-density core that we detected is $\sim$ 50 resolution elements across, indicating that beam-smearing is not responsible for this result. We also calculated the asymmetric drift correction to the rotation curve. Its effect is to increase the maximum disk mass-to-light ratio, and to make the rotation curve slightly more linear, but the density profile does not change significantly.

### 3.3. Comparing Velocities Derived From Different Tracers

Some recent studies in the literature have shown that, beam smearing questions aside, there do not appear to be systematic offsets between H I and H$\alpha$ rotation velocities (e.g., McGaugh, Rubin, & de Blok 2001; Marchesini et al. 2002). With a handful of exceptions, though, these studies employed longslit H$\alpha$ data, so the comparisons essentially took place only along the major axis. In addition, the spatial and velocity resolution of the H I and H$\alpha$ data were often quite different.

Simon et al. (2003) presented for the first time the data necessary for a two-dimensional comparison across a dwarf galaxy of the CO and H$\alpha$ velocity fields. The angular resolution of the two datasets is similar ($6''$ and $4''$, respectively), and although the CO velocity resolution is better by a factor of $\sim 6$, the higher signal-to-noise at H$\alpha$ enables us to measure the velocities with comparable precision. We constructed a unique one-to-one mapping between the two velocity fields. The mean difference between $v_{\rm H\alpha}$ and $v_{\rm CO}$ is 1 km s$^{-1}$ and the rms is 5.3 km s$^{-1}$, with the comparison being made at 173 independent points. Similar studies in the Milky Way found that the dispersion between the velocities of molecular clouds and the associated H$\alpha$-emitting gas was 4-6 km s$^{-1}$ (Fich, Dahl, & Treffers 1990), so much of the scatter we observe between the two in NGC 2976 may be intrinsic to the process of H II region formation rather than caused by observational uncertainties.

This comparison strongly suggests that both the CO and the H$\alpha$ data accurately reflect the gravitational potential of the galaxy, and neither is significantly compromised by systematic effects. Extinction, for example, is not distorting the H$\alpha$ velocity field. If this result can be shown to hold for a few additional galaxies, then it will no longer be necessary to observe more than one velocity field tracer per galaxy. One further test that should be carried out is to compare the velocity field from a gaseous emission-line tracer to that from a stellar absorption-line tracer to assess the agreement between the stellar and gas kinematics. Such studies have been done before (e.g., Mulder 1995; Bottema 1999), but usually only with long-slit observations. Obtaining two-dimensional absorption-line velocity fields is currently observationally challenging but feasible.

### 3.4. Noncircular Motions

Perhaps the most surprising result from Simon et al. (2003) was the finding that NGC 2976 contains strong radial motions. In optical and near-infrared images, the galaxy is very regular, with no hint of a bar or any other deviation from axisymmetry that might affect the kinematics. The finding that the velocity field is clearly different from a purely rotating disk was therefore unexpected. Near the center of the galaxy, the direction of the maximum velocity gradient is up to $\sim 40^\circ$ away from the photometric major axis.

The velocity data can be adequately described by a model in which the galaxy is undergoing circular rotation, but only if the kinematic PA declines monotonically from $\sim 6^\circ$ to $\sim -37^\circ$ over the central kiloparsec. As mentioned above, though, this position angle variation is inconsistent with the photometry. The alternative — and more likely — model is one in which NGC 2976 contains substantial radial flows. The origin of such motions, however, is unclear.

There are several plausible mechanisms for creating radial motions. An intriguing possibility is that the radial motions could be a result of the dark

matter halo having a triaxial rather than spherical shape. CDM halos are expected to be moderately triaxial (e.g., Dubinski & Carlberg 1991; Warren et al. 1992), and the velocity field of a galaxy embedded in a triaxial halo would exhibit noncircular motions. However, since the details of such a velocity field have not yet been investigated with simulations, we cannot compare our results to theoretical predictions. We plan to carry out simulations of the kinematics of a disk within a triaxial halo to see how the halo shape influences the gas kinematics and whether the effect is consistent with the velocity field of NGC 2976. This could become a new technique for measuring the triaxiality of galaxy dark matter halos.

## 4. The Dark Matter Halo of NGC 4605

NGC 4605 is another Sc dwarf galaxy, located at a distance of 4.3 Mpc. Like NGC 2976, it appears to be a pure disk system. We used a long-slit H$\alpha$ spectrum and a two-dimensional CO velocity field to measure its rotation curve (Bolatto et al. 2002). We found that the galaxy probably contains a maximal disk, and that its dark matter density profile goes as $\rho \propto r^{-0.65}$ (see Fig. 3), intermediate between a core and a cusp. The quality of our original observations of NGC 4605 precluded an investigation of the systematics, but we are in the process of analyzing new observations to study their impact.

## 5. The Dark Matter Halo of NGC 5963

NGC 5963 is a more massive ($\sim 10^{10} M_{\odot}$) and more distant ($\sim$ 10 Mpc) galaxy than NGC 2976 and NGC 4605. Its surface brightness profiles are more complicated than those galaxies as well, showing bright emission at the center, surrounded by a transition region in which the surface brightness falls off extremely rapidly (scale length $\approx$ 300 pc), and then a very low surface brightness exponential disk extending from 1.5 kpc out to beyond 3 kpc. The interpretation of this behavior near the center of the galaxy is not straightforward; the galaxy is definitely not strongly barred, but we cannot rule out a bulge component.

### 5.1. Observations

We obtained a two-dimensional H$\alpha$ velocity field of NGC 5963 with the WIYN telescope, using the same technique as for NGC 2976. The spatial resolution of these data is 190 pc and the velocity resolution is 13 km s$^{-1}$. We detected H$\alpha$ emission out to a radius of $\sim$ 3 kpc. We also obtained a two-dimensional CO velocity field from BIMA. The CO emission in this galaxy is limited to the central kiloparsec, but adding the CO data improves our ability to constrain the innermost part of the density profile.

### 5.2. Rotation Curve and Stellar Disk

The combined CO and H$\alpha$ rotation curve of NGC 5963 is displayed in Figure 4. It is immediately clear that the density profile of NGC 5963 has a very different structure from those of NGC 2976 and NGC 4605. Instead of a mostly linear

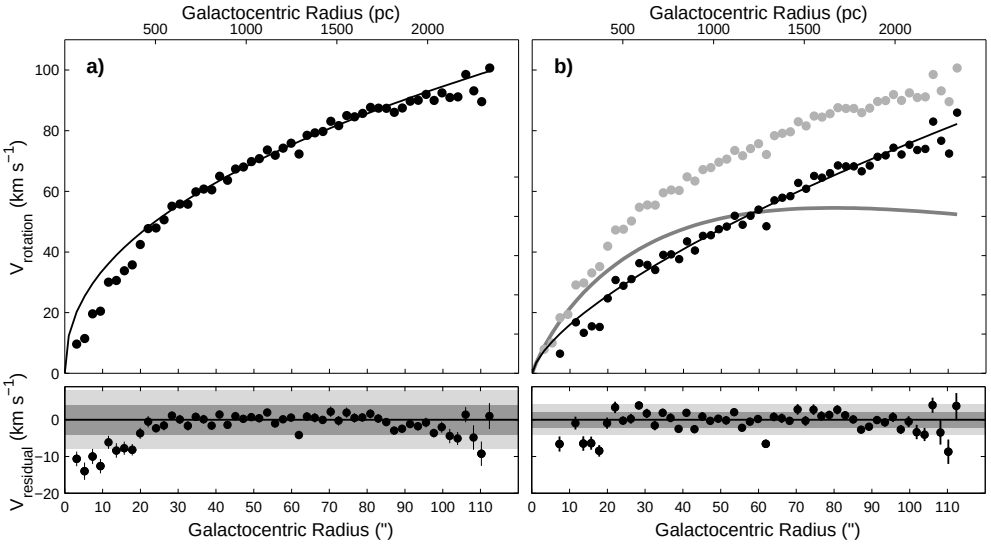


Figure 3. (a) Minimum disk rotation curve of NGC 4605. The black curve is a $\rho \propto r^{-1.1}$ power law fit, which agrees quite closely with the rotation curve beyond 25″. At smaller radii, though, it significantly overestimates the rotation velocities. A separate inner power law ($\rho \propto r^{-0.4}$) is necessary to fit the entire rotation curve. The bottom panel shows the residuals from the fit, with $1\sigma$ and $2\sigma$ departures represented by the shaded regions. Statistical error bars are displayed in the residual plot. (b) Maximum disk rotation curve of NGC 4605. The light gray circles represent the observed rotation curve, and the black circles represent the rotation curve of the dark matter halo after the stellar disk contribution (thick gray curve) has been subtracted. The black curve is a $\rho \propto r^{-0.65}$ power law that provides a good fit to the dark matter rotation curve at all radii.

increase with radius, the rotation curve of NGC 5963 has the classic spiral galaxy shape with a steep inner rise and a nearly flat outer portion.

We perform isophotal fits to the I-band image of NGC 5963 to obtain the shape of its surface brightness profiles. We then calculate the rotation curve due to the stellar disk numerically, as described before. The resulting stellar disk rotation curve can be seen in Figure 4. The maximum disk limit for this galaxy is set by the innermost point of the rotation curve. We derive a maximum disk mass-to-light ratio of $M_*/L_I = 0.7 M_\odot/L_{\odot I}$. Even the maximum disk is unable to account for the observed rotation speed of the galaxy beyond a radius of $\sim 6''$. The calculated value of the maximum disk mass-to-light ratio is not unusually low, so a maximum disk is not required in NGC 5963. The disk can be less massive than shown in Figure 4, but since the galaxy is dark matter-dominated the structure of the dark halo does not depend strongly on the assumed stellar mass-to-light ratio.

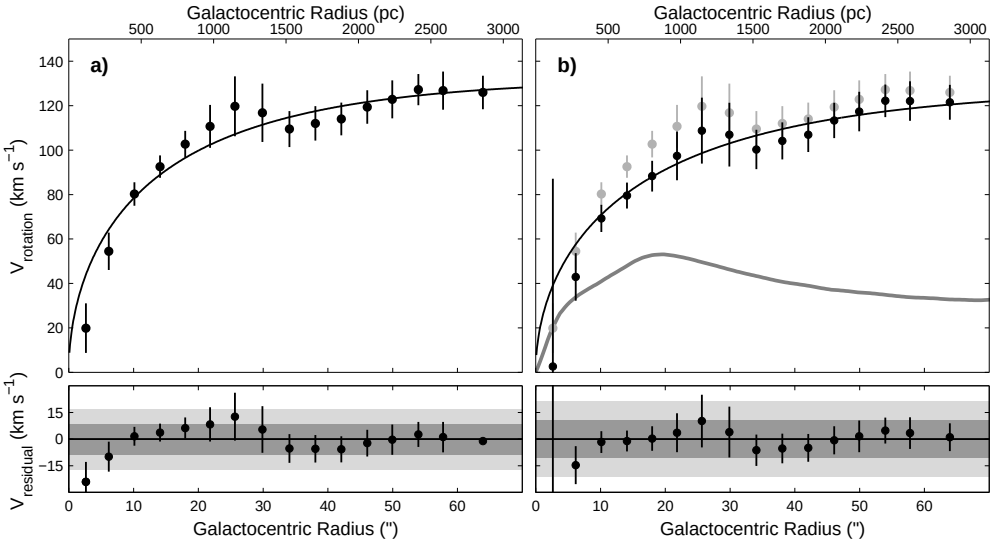


Figure 4. (a) Minimum disk rotation curve of NGC 5963. The black curve shows an NFW fit to the rotation curve with a concentration of 20. Residuals from the fit are plotted in the bottom panel. Unlike the previous two galaxies, a power law is not a very good fit and the NFW form fits much more closely. (b) Maximum disk rotation curve of NGC 5963. Even after removing a maximal stellar disk (thick gray curve; $M_*/L_I = 0.7 M_\odot/L_{\odot I}$), the rotation curve due to the dark matter halo is well-fit by an NFW potential.

### 5.3. Dark Matter Density Profile

Fitting a single power law to the rotation curve of NGC 5963 does not produce a very good fit. The fit is substantially improved by using separate inner and outer power laws, corresponding to an inner density profile of $\rho \propto r^{-1.1}$ and a steeper outer density profile of $\rho \propto r^{-1.4}$. An even better fit can be obtained by fitting an NFW rotation curve to the data; the reduced $\chi^2$ value of this fit is only 1.1. Although the concentration parameter of the halo is not well-constrained, the scale radius is about 3 kpc and the halo has $v_{200} \approx 90$ km s$^{-1}$. An NFW fit can accurately describe the rotation curve for any stellar mass-to-light ratio (see Fig. 4). This galaxy may be the first low-mass system found that contains a density profile that matches the predictions of the numerical simulations.

## 6. Conclusions

We have used high-resolution two-dimensional velocity fields to study the dark matter density profiles of NGC 2976, NGC 4605, and NGC 5963. We showed that these three galaxies contain very different density profiles. For NGC 2976, we presented one of the most detailed velocity fields of a dwarf galaxy outside the Local Group. Even with these high-quality data, we found that NGC 2976 contains a constant-density core and an NFW halo is strongly ruled out. The

dark matter halo of NGC 4605 is intermediate between a constant-density core and a cusp, and NGC 5963 has a cuspy halo that is almost perfectly consistent with an NFW profile.

We conclude that some galaxies do not contain central cusps, even when systematic uncertainties are accounted for as carefully as possible. We also point out that we find no evidence to support the prediction that all dark matter halos share a universal shape. If these results hold as our sample grows, it will demonstrate that the conflict between the observations and the simulations is not caused by systematic problems with the observations. Instead, more effort may be needed to investigate what could be missing from the simulations that would cause them to overestimate density profile slopes.

**Acknowledgments.** This research was supported by NSF grant AST-9981308.

## References

Blais-Ouellette, S., Carignan, C., Amram, P., & Côté, S. 1999, AJ, 118, 2123

Bolatto, A. D., Simon, J. D., Leroy, A., & Blitz, L. 2002, ApJ, 565, 238

Borriello, A., & Salucci, P. 2001, MNRAS, 323, 285

Bottema R. 1999, A&A, 348, 77

Burkert, A. 1995, ApJ, 447, L25

de Blok, W. J. G., Bosma, A., & McGaugh, S. 2003, MNRAS, 340, 657

de Blok, W. J. G., McGaugh, S. S., Bosma, A., & Rubin, V. C. 2001a, ApJ, 552, L23

de Blok, W. J. G., McGaugh, S. S., & Rubin, V. C. 2001b, AJ, 122, 2396

Dubinski, J., & Carlberg, R. G. 1991, ApJ, 378, 496

Fich, M., Dahl, G. P., & Treffers, R. R. 1990, AJ, 99, 622

Flores, R. A., & Primack, J. R. 1994, ApJ, 427, L1

Marchesini, D., D'Onghia, E., Chincarini, G., Firmani, C., Conconi, P., Molinari, E., & Zacchei, A. 2002, ApJ, 575, 801

McGaugh, S. S., Rubin, V. C., & de Blok, W. J. G. 2001, AJ, 122, 2381

Moore, B., Quinn, T., Governato, F., Stadel, J., & Lake, G. 1999, MNRAS, 310, 1147

Mulder, P. S. 1995, A&A, 303, 57

Navarro, J. F., Frenk, C. S., & White, S. D. M. 1996, ApJ, 462, 563 (NFW)

Simon, J. D., Bolatto, A. D., Leroy, A., & Blitz, L. 2003, ApJ, in press (preprint: astro-ph 0307154)

Swaters, R. A., Madore, B. F., van den Bosch, F. C., & Balcells, M. 2003, ApJ, 583, 732 (SMVB)

van den Bosch, F. C., Robertson, B. E., Dalcanton, J. J., & de Blok, W. J. G. 2000, AJ, 119, 1579

van den Bosch, F. C., & Swaters, R. A. 2001, MNRAS, 325, 1017

Warren, M. S., Quinn, P. J., Salmon, J. K., & Zurek, W. H. 1992, ApJ, 399, 405